



# Intracellular O-linked glycosylation directly regulates cardiomyocyte L-type $\text{Ca}^{2+}$ channel activity and excitation–contraction coupling

Andrew R. Ednie<sup>1</sup> · Eric S. Bennett<sup>1</sup>

Received: 8 May 2020 / Accepted: 17 August 2020  
© Springer-Verlag GmbH Germany, part of Springer Nature 2020

## Abstract

Cardiomyocyte L-type  $\text{Ca}^{2+}$  channels ( $\text{Ca}_v$ s) are targets of signaling pathways that modulate channel activity in response to physiologic stimuli.  $\text{Ca}_v$  regulation is typically transient and beneficial but chronic stimulation can become pathologic; therefore, gaining a more complete understanding of  $\text{Ca}_v$  regulation is of critical importance. Intracellular O-linked glycosylation (O-GlcNAcylation), which is the result of two enzymes that dynamically add and remove single N-acetylglucosamines to and from intracellular serine/threonine residues (OGT and OGA respectively), has proven to be an increasingly important post-translational modification that contributes to the regulation of many physiologic processes. However, there is currently no known role for O-GlcNAcylation in the direct regulation of  $\text{Ca}_v$  activity nor is its contribution to cardiac electrical signaling and EC coupling well understood. Here we aimed to delineate the role of O-GlcNAcylation in regulating cardiomyocyte L-type  $\text{Ca}_v$  activity and its subsequent effect on EC coupling by utilizing a mouse strain possessing an inducible cardiomyocyte-specific OGT-null-transgene. Ablation of the OGT-gene in adult cardiomyocytes (OGTKO) reduced OGT expression and O-GlcNAcylation by > 90%. Voltage clamp recordings indicated an ~ 40% reduction in OGTKO  $\text{Ca}_v$  current ( $I_{\text{Ca}}$ ), but with increased efficacy of adrenergic stimulation, and  $\text{Ca}_v$  steady-state gating and window current were significantly depolarized. Consistently, OGTKO cardiomyocyte intracellular  $\text{Ca}^{2+}$  release and contractility were diminished and demonstrated greater beat-to-beat variability. Additionally, we show that the  $\text{Ca}_v \alpha 1$  and  $\beta 2$  subunits are O-GlcNAcylated while  $\alpha 2\delta 1$  is not. Echocardiographic analyses indicated that the reductions in OGTKO cardiomyocyte  $\text{Ca}^{2+}$  handling and contractility were conserved at the whole-heart level as evidenced by significantly reduced left-ventricular contractility in the absence of hypertrophy. The data indicate, for the first time, that O-GlcNAc signaling is a critical and direct regulator of cardiomyocyte  $I_{\text{Ca}}$  achieved through altered  $\text{Ca}_v$  expression, gating, and response to adrenergic stimulation; these mechanisms have significant implications for understanding how EC coupling is regulated in health and disease.

**Keywords** Cardiomyocyte · Voltage-gated  $\text{Ca}^{2+}$  channel · EC coupling · O-GlcNAc · Isoproterenol · Ion channel gating

## Introduction

The transient addition of a single N-acetylglucosamine (GlcNAc) to intracellular serine/threonine residues (O-GlcNAcylation) is a ubiquitous post-translational modification

that contributes to the regulation of a variety of proteins and physiologic processes [29]. O-GlcNAcylation occurs through activity of two enzymes: O-linked  $\beta$ -N-acetylglucosamine transferase (OGT) and O-linked  $\beta$ -N-acetyl glucosaminidase (OGA), which, under normal physiologic conditions, dynamically add and remove GlcNAc residues respectively [29]. Production of the OGT substrate, UDP-GlcNAc, requires processing of metabolites such as glucose, acetyl-coA and glutamine through the hexosamine biosynthesis pathway [50] and was shown to be increased in diabetic conditions [19, 50]; thus, OGT is also often referred to as a nutrient sensor. In addition to those activities common to all cell types including transcription, translation and cellular metabolism [29], O-GlcNAcylation plays an important role in a variety of physiologic processes specific

**Electronic supplementary material** The online version of this article (https://doi.org/10.1007/s00395-020-00820-0) contains supplementary material, which is available to authorized users.

✉ Andrew R. Ednie  
andrew.ednie@wright.edu

<sup>1</sup> Department of Neuroscience, Cell Biology and Physiology, Boonshoft School of Medicine and College of Science and Mathematics, Wright State University, 143 Biological Sciences II, 3640 Colonel Glenn Hwy, Dayton, OH 45435, USA

to cardiomyocyte function including ischemia–reperfusion injury and hypertrophic signaling [4, 20, 39]; however, its role in excitation–contraction (EC) coupling has only recently begun to emerge, and primarily studied only in the context of diabetes/hyperglycemia [9, 13, 19, 31, 52, 53, 55, 68].

L-type voltage-gated  $\text{Ca}^{2+}$  channels ( $\text{Ca}_v$ s), which are putatively formed by the assembly of  $\alpha 1$  ( $\text{Ca}_v1.2$ ),  $\alpha 2\delta 1$  and  $\beta 2$  subunits, trigger cardiomyocyte  $\text{Ca}^{2+}$ -activated  $\text{Ca}^{2+}$ -release and can be directly targeted by signaling pathways that allow the heart to respond to physiologic cues [5, 38]. This modulation of  $\text{Ca}_v$  activity is typically transient and beneficial; however, chronic disease states such as hypertrophic cardiomyopathy and diabetes often appropriate these adaptive signaling pathways such that they become pathologic [8, 22, 38, 59]. Several studies demonstrated that cardiac  $\text{Ca}_v$  activity is depressed in chronic diabetic models [45, 48, 63]; although, the mechanisms are not well understood. Additionally, utilizing a proteomics approach, it was suggested that several neuronal  $\text{Ca}_v$  subunit isoforms bear the O-GlcNAc modification [62]. Despite these findings, a potential role for the regulation of cardiomyocyte  $\text{Ca}_v$ s by O-GlcNAcylation is currently unknown.

Here we sought to determine the inherent functional impact of O-GlcNAcylation on cardiac L-type  $\text{Ca}_v$  activity by utilizing an inducible cardiomyocyte specific OGT-gene deficient mouse strain (OGTKO). Following induction, OGTKO cardiomyocytes demonstrated significant reductions in  $\text{Ca}_v$  current ( $I_{\text{Ca}_v}$ ), with concomitant reductions in  $\text{Ca}_v$   $\alpha 1$  and  $\beta 2$  expression, but with increased efficacy of adrenergic stimulation. OGTKO cardiomyocytes also demonstrated depolarizing shifts in  $\text{Ca}_v$  voltage-dependent steady-state gating. Consistently, intracellular  $\text{Ca}^{2+}$  release and contractility were diminished in OGTKO cardiomyocytes with concurrent reductions in left-ventricular (LV) contractility. We also observed that cardiac  $\text{Ca}_v$   $\alpha 1$  and  $\beta 2$  subunits bear the O-GlcNAc modification, while the  $\alpha 2\delta 1$  subunit does not. Thus, results from this study indicate, for the first time, that O-GlcNAc signaling, under basal and non-diseased related conditions, is a crucial and direct regulator of cardiomyocyte L-type  $\text{Ca}_v$  activity and therefore EC coupling.

## Methods

### Ethical approval

Animals were handled in accordance with the NIH Guide for the Care and Use of Laboratory Animals. All protocols involving animals were approved by the Wright State University Institutional Animal Care and Use Committee. Mice were euthanized, under deep anesthesia (5% isoflurane), by

thoracotomy and excision of the heart to obtain samples for the biochemical and functional studies.

### Generation of the OGTKO and animal use

12–16 week-old male mice were used in all experiments. To create the OGTKO strain, female mice homozygous for a transgene possessing loxP sites flanking the exon encoding amino acids 206–232 of the X-linked OGT gene (004860; The Jackson Laboratory, Bar Harbor, ME, USA) were crossed with male mice possessing one copy of the  $\alpha$ -MHC-MerCreMer transgene, which consists of a cardiac-specific  $\alpha$ -myosin heavy chain promoter directing expression of a tamoxifen-inducible Cre recombinase (005657; The Jackson Laboratory). Cre expression and OGT gene deletion were accomplished by intraperitoneal injection of tamoxifen (75mgs/kg; T5658; MilliporeSigma, Burlington, MA, USA) dissolved in corn oil (C8267; MilliporeSigma) for four consecutive days. To control for potential spurious effects of tamoxifen injection and  $\alpha$ -MHC-MerCreMer expression [6], all control mice were tamoxifen treated and  $\alpha$ -MHC-MerCreMer positive but had a normal OGT gene. Animals were used 18–30 days post induction (dpi).

### Cardiomyocyte isolation

Cardiomyocytes from the LV wall were isolated using 1 mg/ml collagenase type II (CLS2; Worthington Biochemical, Lakewood, NJ, USA) and 0.65 u/ml protease XIV (P5147; MilliporeSigma) via Langendorff perfusion as previously described [15, 17]. Myocytes were stored in a modified Hank's balanced salt solution buffered with 10 mmol/liter (mM) (4-(2-hydroxyethyl)-1-piperazineethanesulfonic acid (HEPES) and supplemented with 1× essential amino acids (11130051; Thermo Fisher Scientific, Waltham, MA, USA) at room temperature. Myocytes were used 1–6 h following isolation.

### Electrophysiology

$\text{Ca}_v$  activity was recorded at room temperature using the whole-cell patch clamp technique as previously described [14, 15]. Briefly, myocytes were added to a recording chamber and bathed in a solution consisting of the following in mM: 136  $\text{NaCl}$ , 1  $\text{MgCl}_2$ , 1  $\text{CaCl}_2$ , 10 glucose, 10 HEPES, 4  $\text{CsCl}$ , 0.02 tetrodotoxin; pH 7.4. Cells were ruptured following seal formation and dialyzed (5 min) with an intracellular recording solution (in mM): 110  $\text{Cs}^+$  methanesulfonate, 30  $\text{CsCl}$ , 10 HEPES, 0.5  $\text{CaCl}_2$ , 2  $\text{MgCl}_2$ , 5  $\text{Na}_2\text{ATP}$ , 5 EGTA; pH 7.2. Cells were voltage clamped at  $-50$  mV and cell size was determined by integrating the capacitance of the cell following a 25 ms, 10 mV step in voltage. Series resistance was

compensated to a minimum of 80%. Analog signals were low-pass filtered (5 kHz) then digitized (50 kHz) and voltage clamp protocols were written and executed using Clampex 10.6 (Molecular Devices, Sunnyvale, CA, USA). Leak currents were always fewer than 50 pA and were ignored.

To record  $I_{Ca}$ , cells were clamped at  $-50$  mV then depolarized by a series of voltage steps beginning at  $-40$  mV and ending at  $60$  mV for  $1.2$  s in  $10$ -mV increments. The voltage steps were separated by  $15$  s. The maximum negative current at each test pulse was divided by capacitance for each cell and averaged to report the current-density/voltage relationships. The rate of fast inactivation was determined by fitting the decay portion of a current trace elicited from a test pulse to  $20$  mV with a bi-exponential function. To calculate conductance, the maximum negative current was divided by the driving force as described [14, 15]. The reversal potential was determined empirically for each cell and was not different between groups. Conductance/voltage relationships were fit with a single Boltzmann function as described to determine activation/gating parameters [14, 15].

To measure  $Ca_v$  voltage-dependent inactivation, cells were held at  $-50$  mV and subjected to conditioning voltage pulses ranging from  $-60$  to  $10$  mV in  $10$  mV increments for  $400$  ms. Following the conditioning pulses, the cells were depolarized to  $20$  mV for  $400$  ms. Each sweep was separated by  $15$  s. The maximum negative amplitude from each current trace was normalized to the maximum negative amplitude from the first step to  $20$  mV. The data were fit with a single Boltzmann function as described [14, 15].

To determine the efficacy of  $\beta$  adrenergic activation on  $Ca_v$  activity, myocytes were clamped at  $-50$  mV and depolarized to  $10$  mV every  $30$  s as  $1$   $\mu$ M of the  $\beta$  adrenergic agonist isoproterenol was perfused through the recording chamber. Isoproterenol was shown to induce a hyperpolarizing shift in  $Ca_v$  activation [44]; therefore, a  $10$  mV test pulse was used since this was close to the saturating voltage of the GV curve (Fig. 2d) yet still elicited a measurable current from OGTKO myocytes. Current from each test pulse was normalized to the current elicited from the initial test pulse at the start of the perfusion.

## Western blotting and antibodies

Total protein was isolated from OGTKO and control ventricles by homogenization in HEPES buffered saline supplemented with  $1\%$  amidosulfobentaine,  $1\times$  Complete Ultra protease inhibitor cocktail (5892970001; Roche, Mannheim, DE),  $0.01$  calpain inhibitors I and II (A2602 and A2603; Apex Bio, Houston, TX, USA),  $0.001$  thiamet G (13237; Caymen Chemical, Ann Arbor, Michigan, USA) and  $0.02\%$   $Na^+$  azide. In the studies investigating ubiquitination,  $100$  mM N-ethylmaleimide was included in the lysis buffer [18]. Protein lysates were Western blotted as

previously described using a bis-tris based buffer system and gels containing an acrylamide/bis-acrylamide ratio of  $49:1$  to facilitate transfer of the large  $Ca_v\alpha 1$  and  $\alpha 2\delta 1$  proteins [14–17]. Immunodetection was performed using the following commercially-available antibodies: anti- $Ca_v1.2$ , anti- $Ca_v\beta 2$ , anti- $Ca_v\alpha 2\delta 1$  (ACC-003, ACC-105 and ACC-015 respectively; Alomone, Jerusalem, IL), anti-OGT, anti-mono/poly ubiquitin (24083 and 3936 respectively; Cell Signaling, Danvers, MA, USA), RL-2 (MA1-072; Thermo Fisher Scientific), anti-NEDD4-1 (611480; BD, San Jose, CA, USA), goat anti-rabbit IgG-horseradish peroxidase (HRP; AP307P; MilliporeSigma) and goat anti-mouse IgG-HRP (AP308P; MilliporeSigma). HRP signals were normalized to total protein staining by addition of  $2,2,2$ -trichloroethanol to the resolving gel to calculate relative protein expression between OGTKO and controls as described [15, 17]. Image analysis was performed in ImageLab (Bio-Rad Laboratories, Hercules, CA, USA) and Western figures are presented as merged files consisting of the chemiluminescent and colorimetric data to show the molecular weight markers.

## Whole-cell $Ca^{2+}$ signaling and myocyte contractility measurements

LV myocytes were stained with fura-2AM and the dye was allowed to de-esterify. Stained myocytes were stimulated with  $20$  volts at  $1$  Hz (MyoPacer; IonOptix, Westwood, MA, USA) and  $Ca^{2+}$  transients were recorded ratiometrically all as previously described [15, 17]. Myocyte contraction was recorded independently by edge detection of unloaded cardiomyocytes at  $250$  Hz [15]; contraction was induced by stimulation as described above.  $Ca^{2+}$  signals and myocyte contraction were analyzed with FelixGX (PTI; Horiba Scientific, Edison, NJ, USA) and IonWizard 7.4 (IonOptix, Westwood, MA, USA) to compare standard parameters including max slope, time-to-peak,  $Ca^{2+}$  transient duration, activation/inactivation kinetics and fractional shortening; these parameters were calculated as the mean of ten consecutive stimulation events that followed ten unrecorded events to ensure complete SR loading. Whole-cell  $Ca^{2+}$  signals and contractility measurements were made at room temperature.

## O-GlcNAc affinity precipitation

Protein was extracted as described above and preabsorbed with streptavidin coated magnetic beads (88816; Thermo Fisher Scientific) for  $\sim 2$  h at  $4$  °C. To capture proteins with the O-GlcNAc modification, biotinylated succinylated wheat germ agglutinin (sWGA; B-1025S; Vector Laboratories, Burlingame, CA, USA) was coupled to the streptavidin magnetic beads. Following preabsorption, protein was added to the lectin coupled beads and mixed overnight at  $4$  °C, washed extensively with lysis buffer and eluted in  $1\times$ LDS-PAGE

sample buffer at 60 °F for 5 min. To ensure specificity, parallel experiments were always performed where sWGA was preabsorbed with 500 mM GlcNAc during the bead/lectin coupling and 50 mM during protein/bead incubations. Following elution, eluates were Western blotted as described above.

## Echocardiography

Transthoracic echocardiography was performed using a Vevo 3100 (Fujifilm, Japan) equipped with a digital transducer centered on 30 MHz (20–46 MHz). Mice were anesthetized with ~2.0–2.5% isoflurane/O<sub>2</sub>. B and M mode images were acquired digitally and analyzed using VevoLab 3.1 (VisualSonics) to compare standard hemodynamic parameters as described by us previously [12, 15]. Briefly, 2-D mode in parasternal long axis and the parasternal short axis at the mid-papillary muscle level were imaged. From this parasternal short axis view, the 2-D guided M mode across the anterior and posterior wall were recorded and LV anterior wall thickness at diastole and systole (LVAW<sub>d</sub> and LVAW<sub>s</sub>, respectively) and LV posterior wall thickness at diastole and systole (LVPW<sub>d</sub> and LVPW<sub>s</sub>, respectively) were measured. Using the leading edge method, all other parameters including ejection fraction (EF) and fractional shortening (FS) were measured from three consecutive cardiac cycles according to the guidelines of the American Society of Echocardiography [40] and as described by us previously [12, 15].

## Statistical analysis

Data are presented as mean  $\pm$  SEM and significance was determined using unpaired student's t-tests and Mann–Whitney rank sum tests where appropriate with a *p* criteria of  $<0.05$ . Animal numbers are listed as "N" and cell numbers as "n". All data are available upon request.

## Results

### Cardiomyocyte deletion of the OGT gene reduces OGT and O-GlcNAcylation levels by at least 90%

To assess the amount to which induced cardiomyocyte deletion of the OGT gene diminishes OGT expression, Western analysis was performed on ventricular protein lysates and indicated a nearly 90% reduction in OGTKO OGT (Fig. 1a and c; *N* = 3; *p* = 0.001). To determine the levels to which O-GlcNAcylation was reduced in OGTKO cardiomyocytes, the monoclonal antibody RL-2, which

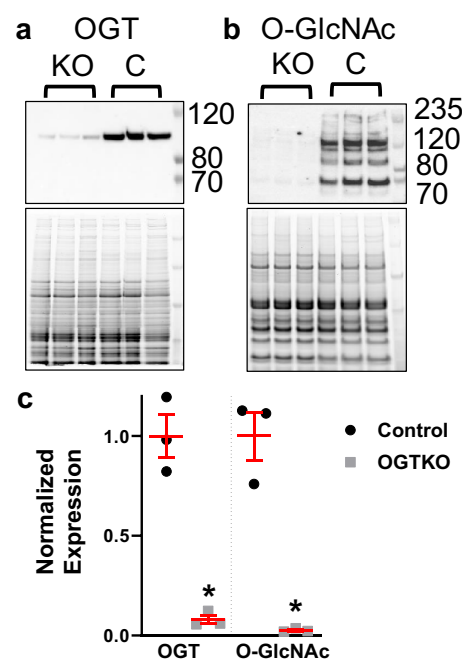


**Fig. 1** Cardiomyocyte OGT-gene deletion significantly reduces OGT and O-GlcNAc levels. **a, b** Western and immunodetection analysis (upper panels) indicated that, following tamoxifen induction, OGTKO (KO; gray squares) ventricular OGT expression and LV myocyte O-GlcNAcylation are markedly reduced compared to controls (c; black circles). Signals were normalized to total protein levels (lower panels). Molecular weights in kilodaltons are listed on the right. **c** Mean  $\pm$  SEM normalized OGT and O-GlcNAcylation signals (*N* = 3; \**p* = 0.001; *t*-test)

recognizes O-GlcNAcylated serine/threonine residues with only some other peptide dependence [61], was used and indicated an ~97% reduction in OGTKO cardiomyocyte O-GlcNAcylation (Fig. 1b and c; *N* = 3; *p* = 0.001). These results demonstrated that, following induction, OGT gene deletion markedly reduces OGT expression and cardiomyocyte O-GlcNAcylation.

### Ca<sub>v</sub> activity is diminished with chronic reductions in O-GlcNAcylation, while adrenergic efficacy is increased

To investigate whether reductions in O-GlcNAcylation affect Ca<sub>v</sub> activity, we compared whole-cell LV cardiomyocyte *I*<sub>Ca</sub> from OGTKO and control animals (Fig. 2a). As discussed in the Methods, here and throughout, all control animals were  $\alpha$ -MHC-MerCreMer positive, were administered tamoxifen, but possessed a normal OGT gene; thereby, controlling for any effects of tamoxifen-treatment and Cre expression. OGTKO cardiomyocytes demonstrated significant reductions in *I*<sub>Ca</sub> density at all channel-activating test

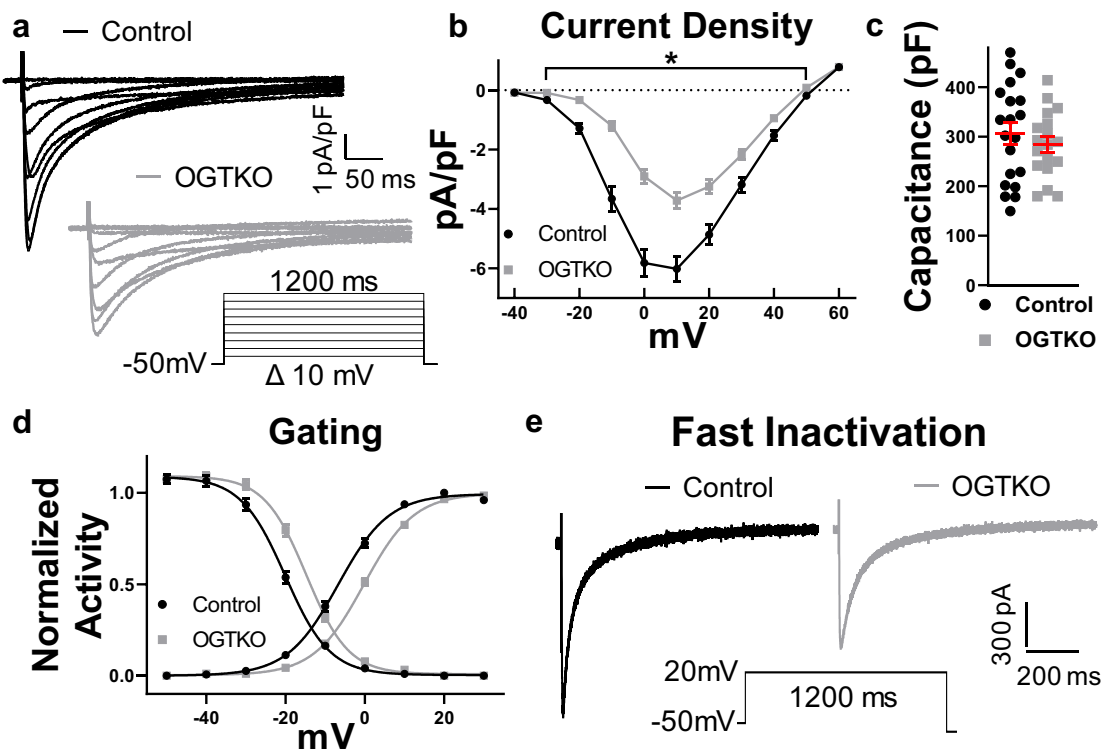


**Fig. 2**  $\text{Ca}_v$  activity is diminished, gating depolarized and inactivation slowed in OGTKO LV myocytes. **a** Representative whole-cell voltage-sensitive  $\text{Ca}^{2+}$  current ( $I_{\text{Ca}}$ ) density traces recorded from control (black) and OGTKO (gray) LV myocytes. **b** Current density–voltage relationships indicated significant reductions in OGTKO current densities. **c** Cell size measured as capacitance was not different

between groups. **d**  $\text{Ca}_v$  voltage-dependent gating and window current were significantly depolarized by 5–6 mV in OGTKO LV myocytes. **e** The rates of the fast and slow components of  $\text{Ca}_v$  inactivation were significantly slower in OGTKO myocytes. **a–e**  $N=3–4$ ;  $n=18–20$ ;  $*p\leq 0.04$ ;  $t$ -test

potentials with no effect on reversal potential (Fig. 2b). For example, at a test potential of 10 mV, OGTKO  $I_{\text{Ca}}$  density was reduced by 38% compared to controls [Fig. 2b and supplemental Table 1 (ST1);  $p < 0.0001$ ; for all  $I_{\text{Ca}}$  parameters:  $N=3–4$ ;  $n=18–20$ ]. Cell capacitances were statistically the same between groups (Fig. 2c and ST1). The voltage-dependence of  $\text{Ca}_v$  steady-state gating was determined and indicated nearly uniform depolarizing shifts of 5–6 mV for voltage-dependent inactivation and activation respectively, including rightward shifts in the activation and inactivation midpoints but with no effect on the slope of the Boltzmann fits (Fig. 2d and ST1;  $p \leq 0.001$ ). To determine the rate of fast inactivation, current traces elicited from a 20 mV test pulse were fit with a bi-exponential function. A 20 mV test potential was utilized because this voltage occurred at a saturating point of the GV curve (Fig. 2d) so that the inherent effect of a rightward shift in voltage-dependent activation, as observed in OGTKO myocytes, would not influence the measurement of inactivation rate. Both the slow and fast components of  $\text{Ca}_v$  inactivation were significantly slower in OGTKO cardiomyocytes by 14 and 36% respectively (Fig. 2e and ST1;  $p \leq 0.03$ ;  $N=3–4$ ;  $n=18–20$ ).

A requisite function of cardiac L-type  $\text{Ca}_v$ s is response to increased sympathetic drive through activation of cardiomyocyte adrenergic receptors resulting in increased  $I_{\text{Ca}}$  [38]. To test whether OGTKO  $\text{Ca}_v$ s respond normally to adrenergic activation, cardiomyocyte  $\text{Ca}_v$  activity was recorded before and after perfusion with 1  $\mu\text{M}$  of the  $\beta$ -adrenergic receptor agonist isoproterenol. Myocytes were voltage-clamped at  $-50$  mV and depolarized to a near-saturating 10 mV test pulse every 30 s during the perfusion. Results from these experiments indicated that isoproterenol induced a robust increase in  $I_{\text{Ca}}$  in both control and OGTKO myocytes (Fig. 3e and f); however,  $I_{\text{Ca}}$  from OGTKO myocytes demonstrated a 51% larger increase following isoproterenol treatment compared to controls (Fig. 3c and ST1; ~1.8 versus 2.7-fold difference;  $N=3–4$ ;  $n=7–8$ ;  $p=0.02$ ). Despite the increased efficacy of isoproterenol on OGTKO  $\text{Ca}_v$ s, following isoproterenol treatment, OGTKO  $I_{\text{Ca}}$  was still ~20% lower than control  $I_{\text{Ca}}$  under basal conditions suggesting that the dysregulation of adrenergic signaling was not solely responsible for the decrease in basal OGTKO  $I_{\text{Ca}}$ .

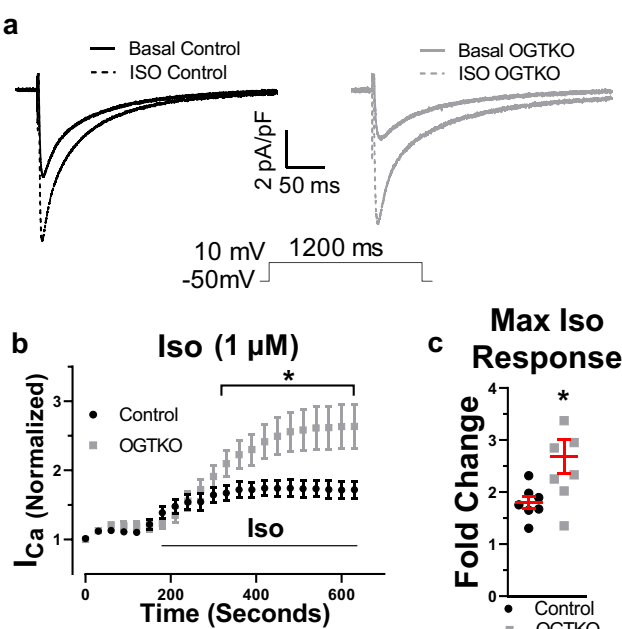


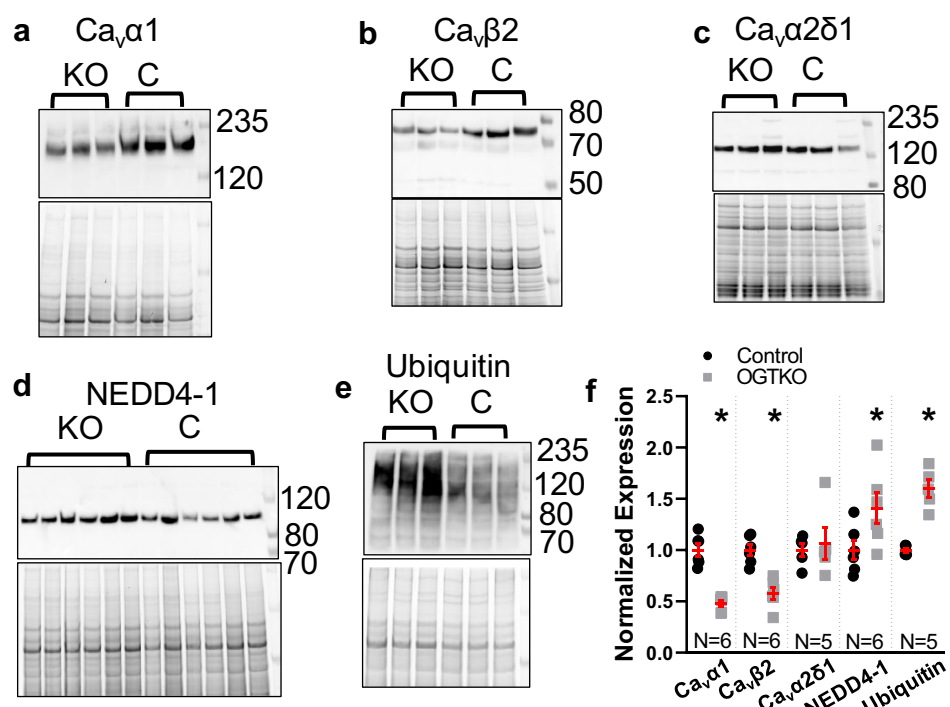
**Fig. 3** The efficacy of isoproterenol on  $I_{Ca}$  is heightened in OGTKO LV myocytes. **a** Representative  $I_{Ca}$  density traces following control perfusion (basal) and perfusion with 1  $\mu$ M isoproterenol (ISO). **b** Scatter plots of perfusion time with 1  $\mu$ M ISO versus normalized current indicating increased efficacy of adrenergic stimulation on OGTKO  $Ca_v$ . **c** Mean  $\pm$  SEM maximum fold change of  $I_{Ca}$  following perfusion with 1  $\mu$ M ISO. **b** and **c**:  $N=3-4$ ;  $n=7-8$ ;  $*p \leq 0.04$ ;  $t$ -test

### $Ca_v \alpha 1$ and $\beta 2$ protein levels are reduced in OGTKO hearts with $\alpha 2 \delta 1$ levels unaffected

To test whether the observed reduction in OGTKO  $I_{Ca}$  density was caused by a decrease in the number of functional  $Ca_v$ , Western analysis was performed on cardiac protein lysates using antibodies that recognize the three putative cardiac  $Ca_v$  subunits.  $Ca_v \alpha 1$  and  $\beta 2$  expression, but not  $\alpha 2 \delta 1$ , were significantly reduced in OGTKO ventricles by 52 and 42% respectively (Fig. 4a–c and f;  $N=6$ ;  $p \leq 0.0004$ ). Under these experimental conditions, only the truncated  $\alpha 1$  form was detected, which was shown to represent at least 80% of the total  $\alpha 1$  protein pool in cardiac tissue [1, 36] and can migrate in SDS-PAGE conditions through a range of apparent molecular weights (~175 kDa to ~210 kDa) largely depending on the extent of processing and the acrylamide concentration and acrylamide/bis-acrylamide ratio [11, 24, 28]. The specificities of all  $Ca_v$  subunit antibodies were tested using their respective immunizing peptides provided by the manufacturer of the antibodies.

Expression system studies previously showed that the ubiquitin ligase, neuronal precursor cell-expressed developmentally down-regulated 4 isoform 1 (NEDD4-1), down-regulates expression and activity of the L-type  $Ca_v$  [56]. It was also shown that O-GlcNAcylation negatively regulates NEDD4-1 expression [34]. We therefore rationalized that NEDD4-1 would be upregulated in OGTKO cardiomyocytes and this might contribute to the observed  $Ca_v$  downregulation. Western analysis indicated that, indeed, NEDD4-1 expression levels were 41% higher in OGTKO

**Fig. 4**  $Ca_v \alpha 1$  and  $\beta 2$  expression are decreased, NEDD4-1 expression and protein ubiquitination are increased, and  $Ca_v \alpha 2 \delta 1$  levels are similar in OGTKO ventricles. **a–e** Western and immunodetection results (top panels) from OGTKO (KO; gray squares) and control (C; black circles) ventricular protein lysates. Molecular weights in kilodaltons are listed on the right. Optical densities were normalized to total protein levels (bottom panels). **f** Mean  $\pm$  SEM normalized expression levels.  $N=5-6$ ;  $*p < 0.05$ ;  $t$ -test



hearts (Fig. 4d and f;  $N=6$ ;  $p<0.05$ ). A major function of NEDD4-1 is to ubiquitinate proteins which targets them for degradation [32]. While the study by Rougier et al. suggested that the regulation of L-type  $\text{Ca}_v$ s by NEDD4-1 overexpression did not involve increased  $\text{Ca}_v1.2$  ubiquitination [56], interest remained in determining whether ubiquitination levels were altered in OGTKO hearts, which would be consistent with increased NEDD4-1 expression. To test this, blotted protein was subjected to immuno-detection using an antibody that recognizes mono- and poly-ubiquitinated proteins; the data indicated that protein ubiquitination was increased by 60% in OGTKO hearts (Fig. 4e and f;  $N=5$ ;  $p=0.008$ ).

### $\text{Ca}_v\alpha 1$ and $\beta 2$ subunits are O-GlcNAcylated but the $\alpha 2\delta 1$ subunit is not

To investigate whether  $\text{Ca}_v$  subunits are directly O-GlcNAcylated, we performed affinity precipitation with biotinylated sWGA that was coupled to streptavidin-coated magnetic beads. sWGA binds terminal GlcNAc residues and can be used to precipitate O-GlcNAcylated proteins [46]. In some previous cases, affinity reagents that recognize the O-GlcNAc modification were shown to cross-react with extracellular N-glycans that possess terminal GlcNAcs [54]. Unlike here, this is often not a limitation because most proteins studied in the context of O-GlcNAcylation are nucleocytoplasmic and are typically not N-glycosylated. The  $\alpha 2\delta 1$  subunit is heavily N-glycosylated and, while it does not appear to occur at high levels, it is possible that the cardiac  $\alpha 1$  subunit is N-glycosylated as well [15];  $\beta 2$  is cytosolic. To overcome the potential spurious reactivity of  $\alpha 1$  and/or  $\alpha 2\delta 1$  terminal N-linked GlcNAcs with sWGA, we utilized a mouse model developed by our lab where hybrid/complex N-glycosylation, and therefore the addition of terminal N-linked GlcNAcs, cannot occur (MGAT1KO) [15, 17]. Detergent soluble protein lysates from MGAT1KO hearts were subjected to sWGA precipitation and indicated that both the  $\alpha 1$  and  $\beta 2$  subunits were precipitated by sWGA while  $\alpha 2\delta 1$  was not (Fig. 5). Similar experiments were performed using protein lysates from OGTKO and control ventricles (not shown). Precipitation of  $\text{Ca}_v\alpha 1$  and  $\beta 2$  by sWGA in control lysates was identical to that which was precipitated from MGAT1KO lysates with only marginal pull-down observed in OGTKO lysates, which was likely the result of spurious reactivity as described above, non-specific binding, and/or residual OGT expression. Together, these data, along with the functional data (Fig. 2), offer strong evidence that  $\text{Ca}_v\alpha 1$  and  $\beta 2$  are directly O-GlcNAcylated under basal conditions and that this modification is an important regulator of  $\text{Ca}_v$  function.

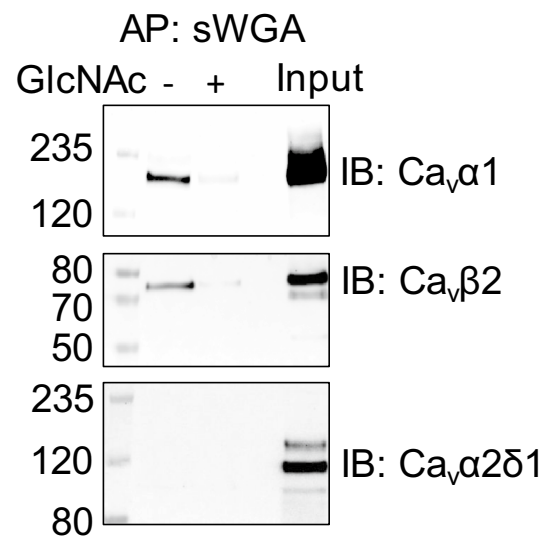
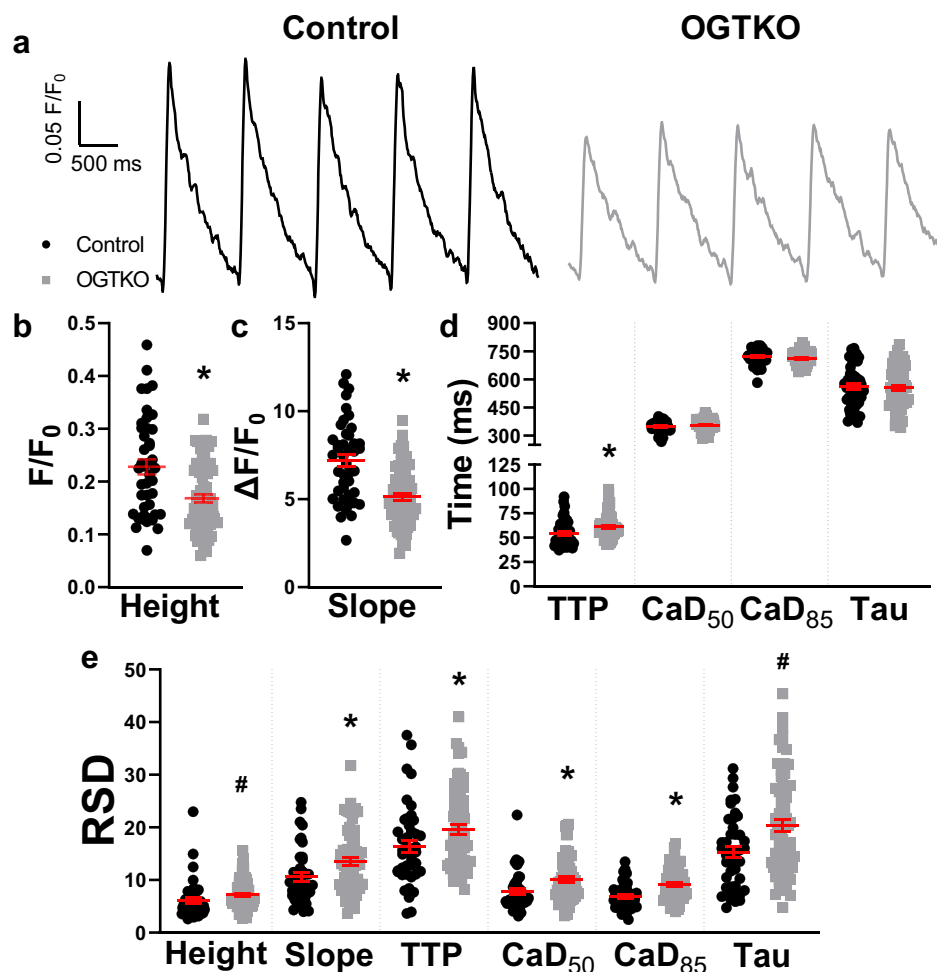


**Fig. 5**  $\text{Ca}_v\alpha 1$  and  $\beta 2$  are O-GlcNAcylated but  $\text{Ca}_v\alpha 2\delta 1$  is not. Affinity purification (AP) using the lectin sWGA, which recognizes terminal GlcNAc residues, was performed in the presence (+) or absence (−) of 500 mM N-acetylglucosamine (GlcNAc). GlcNAc was used to demonstrate specificity as free excess GlcNAc would saturate binding of the lectin and prevent precipitation of O-GlcNAcylated proteins by the bead-lectin sorbent. Precipitated protein eluates were subjected to Western and immunoblot (IB) analysis using  $\text{Ca}_v$  subunit specific antibodies and results indicated that sWGA precipitates  $\text{Ca}_v\alpha 1$  and  $\beta 2$  but not  $\text{Ca}_v\alpha 2\delta 1$ . Images are representative of 5–6 independent experiments

### Intracellular $\text{Ca}^{2+}$ release and contractility are diminished and more variable in OGTKO myocytes

In cardiomyocytes,  $I_{\text{Ca}}$  is the primary trigger for release of  $\text{Ca}^{2+}$  from intracellular stores [60]. Therefore, to test whether the reductions in OGTKO  $\text{Ca}_v$  activity impact intracellular  $\text{Ca}^{2+}$  release, we performed fura-2 ratiometric  $\text{Ca}^{2+}$  photometry in field-stimulated (1 Hz/20 volts) OGTKO and control LV myocytes (Fig. 6a). OGTKO myocytes demonstrated an ~ 27% decrease in the magnitude and rate of intracellular  $\text{Ca}^{2+}$  release and a 12% slowing in the time-to-peak (TTP) of the  $\text{Ca}^{2+}$  transient (Fig. 6b–d). Contrastingly,  $\text{Ca}^{2+}$  transient duration and rate of decay, which are indicators of the time required for intracellular  $\text{Ca}^{2+}$  to be extruded or re-sequestered, were not different between groups (Fig. 6d; for all  $\text{Ca}^{2+}$  transient parameters:  $N=3$ ;  $n=43–66$ ;  $p\leq 0.003$  where significant). The robust effects on  $\text{Ca}^{2+}$  transient activation with no observed effects on  $\text{Ca}^{2+}$  transient duration or relaxation suggest that the reduction in OGTKO  $I_{\text{Ca}}$  density contributes to the diminished  $\text{Ca}^{2+}$ -activated  $\text{Ca}^{2+}$ -release observed in OGTKO LV myocytes although this does not rule out an effect of reductions in O-GlcNAc levels on ryanodine receptor activity. These data also suggest that, while phospholamban was shown to be O-GlcNAcylated [68], prevention of O-GlcNAcylation under basal conditions does

**Fig. 6** The magnitude and kinetics of intracellular  $\text{Ca}^{2+}$  release are reduced and more variable in OGTKO LV myocytes with no measurable effect on  $\text{Ca}^{2+}$  re-sequestration or efflux. **a** Representative fura-2 ratiometric  $\text{Ca}^{2+}$  transients recorded from control (black) and OGTKO (gray) LV myocytes. **b–d** Mean  $\pm$  SEM  $\text{Ca}^{2+}$  transient parameters for control (black circles) and OGTKO (gray squares) LV myocytes. **e** The relative standard deviation (RSD) of  $\text{Ca}^{2+}$  handling parameters were calculated by normalizing each parameter's standard deviation from ten consecutive  $\text{Ca}^{2+}$  transients by their respective means and indicated greater variability in OGTKO myocytes. For all  $\text{Ca}^{2+}$  handling parameters:  $N=3$ ;  $n=43–66$ ;  $*p\leq 0.03$ ,  $t$ -test;  $^{\#}P\leq 0.009$ , Mann–Whitney rank sum test. TTP: time-to-peak;  $\text{CaD}_{50-85}$ :  $\text{Ca}^{2+}$  transient duration at 50 and 85% return-to-baseline values; Tau: single exponential  $\text{Ca}^{2+}$  transient inactivation time constant



not measurably impact the role of phospholamban in  $\text{Ca}^{2+}$  re-sequestration.

To determine whether the decrease in OGTKO  $\text{Ca}^{2+}$ -activated  $\text{Ca}^{2+}$ -release could impact contractility, we assessed sarcomere shortening of unloaded and field stimulated (1 Hz/20 volts) LV myocytes from OGTKO and control hearts (Fig. 7a and b). Fractional shortening was significantly reduced, and the rate of shortening was slowed, each by  $\sim 40\%$  in OGTKO myocytes, with no significant effect on relaxation kinetics (Fig. 7c and d;  $N=3$ ;  $n=18–29$ ;  $p\leq 0.04$ ). In addition to the reductions in myocyte contraction, it was apparent that OGTKO fractional shortening demonstrated significantly greater beat-to-beat variability compared to controls (Fig. 7a and b). To quantify this, the relative standard deviations of ten consecutive contractions were compared between groups. Strikingly, the variability in contractile parameters from rhythmic contractions was  $\sim 78–177\%$  greater in OGTKO myocytes compared to controls (Fig. 7e;  $N=3$ ;  $n=18–29$ ;  $p\leq 0.02$ ). A similar analysis was performed on the recorded  $\text{Ca}^{2+}$  transients (Fig. 6) and while the magnitude of variability was not as large as what was observed for contractility, all OGTKO

$\text{Ca}^{2+}$  transient parameters demonstrated significantly greater variability than controls (18–33%; Fig. 6e;  $N=3$ ;  $n=43–66$ ;  $p\leq 0.03$ ).

#### The deficits in OGTKO cardiomyocyte contractility are conserved at the whole-heart level

To determine whether the reductions and increased variability of myocyte  $\text{Ca}^{2+}$  handling and contractility were conserved at the whole-heart level, echocardiography of the LV was performed on OGTKO and control animals pre-induction (baseline) then again at 19 dpi (the time at which the myocyte  $\text{Ca}^{2+}$  transient and contractility measurements were made), and at 29 dpi. At 19 dpi, EF and FS were significantly reduced by  $\sim 37$  and 45% respectively in OGTKO animals compared to baseline levels with consistent increases in end systolic volumes (ESV) and internal LV dimension at systole ( $[(\text{LVID}_s)]$  Fig. 8 and ST2;  $N=7$ ;  $p\leq 0.04$ ). There were, however, no changes in wall thickness, end-diastolic volume (EDV) or internal dimensions ( $\text{LVID}_d$ ) that would indicate hypertrophy (ST2); this is consistent with the similar OGTKO and control cell sizes as indicated through

**Fig. 7** OGTKO LV myocyte contractility is diminished and more variable. **a, b** Representative cell shortening from control (black) and OGTKO (grey) field-stimulated (20 volts/1Hz) LV myocytes. **c, d** Mean  $\pm$  SEM fractional shortening (FS) and contraction (contract)/relaxation (relax) kinetics (change in length/time;  $\Delta L/\Delta T$ ) for control (black circles) and OGTKO (gray squares) LV myocytes. **e** Relative standard deviation (RSD) of FS and contractile kinetics.  $N=3$ ;  $n=18-29$ ; \* $p\leq 0.04$ ;  $t$ -test

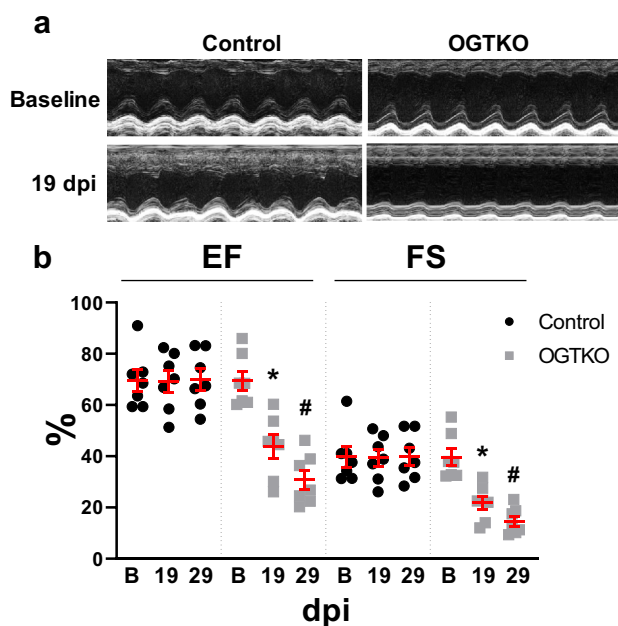
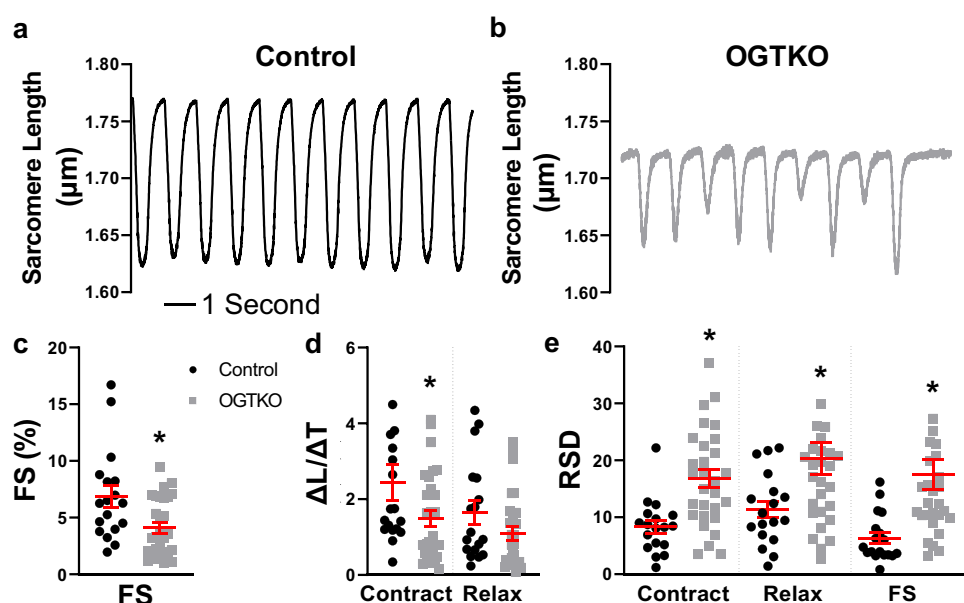


**Fig. 8** OGTKO LV contractility is reduced concurrent with diminished myocyte EC coupling and worsens over time. **a** Representative M mode images taken from control (left) and OGTKO (right) left ventricles at pre-induction (baseline; top) and 19 days post induction (dpi; bottom). **b** Mean  $\pm$  SEM scatter plots of LV ejection fraction (EF) and fractional shortening (FS) parameters measured from echocardiographs of control (black circles) and OGTKO (gray squares) hearts at baseline (B), 19 and 29 dpi.  $N=7$ ; \* $p=0.01$ : 19 dpi versus B; # $p=0.01$ : 29 dpi versus 19 dpi

membrane capacitance measurements (Fig. 2c). The loss of contractility was progressive in that at 29 dpi, OGTKO EF and FS were further reduced by  $\sim 30$  and 33% respectively compared to 19 dpi (Fig. 8b and ST2;  $N=7$ ;  $p=0.01$ ). At

29 dpi, compared to baseline values, an  $\sim 23\%$  reduction in OGTKO LVPWs was observed with no other changes in wall thicknesses (ST2;  $N=7$ ;  $p=0.04$ ) suggesting that OGTKO animals forego any hypertrophy and enter directly into heart failure. Control animals showed no significant change in any recorded parameter at any time point tested, and at baseline, all measured parameters showed no difference in systolic function between OGTKO and control hearts (Fig. 8 and ST2;  $N=7$ ). Together, these data strongly suggest that the EC coupling and contractile dysfunctions conferred by OGT deletion in cardiomyocytes and described in Figs. 6 and 7 translate directly to aberrant LV shortening and contractility with no indication of hypertrophy at the cellular or LV levels.

## Discussion

Here we show that chronic reductions in cardiomyocyte O-GlcNAcylation significantly impact  $\text{Ca}_v$  function. We observed reductions in OGTKO  $I_{\text{Ca}}$  density, with no impact on cell size, and consistent decreases in  $\text{Ca}_v \alpha 1$  and  $\beta 2$  expression. Further, the data showed increased efficacy of adrenergic stimulation on OGTKO  $\text{Ca}_v$ . We also observed rightward shifts in OGTKO  $\text{Ca}_v$  steady-state gating. Together, the data show that reduced O-GlcNAc levels impact  $\text{Ca}_v$  through at least three previously undescribed mechanisms: (1) reduced  $\text{Ca}_v$  subunit expression, (2) depolarizing shifts in  $\text{Ca}_v$  steady-state gating and window current, and (3) increased adrenergic stimulation efficacy. Furthermore, while it is not possible at this time to rule out a contribution of aberrant contractile protein function, some of which were shown to be dynamically O-GlcNAcylated [52],

53], or dysregulation of intracellular  $\text{Ca}^{2+}$  handling proteins, the observed reductions and increased variability in  $\text{Ca}^{2+}$  handling and contractility are consistent with reduced and altered  $\text{Ca}_v$  function including the observed rightward shift in OGTKO  $\text{Ca}_v$  window current and slowing of inactivation (Fig. 2d and e) suggesting a critical role for O-GlcNAcylation in these processes. Finally, the severe impact of OGT gene deletion on cardiomyocyte EC coupling is observed at the whole-heart level as evidenced by the concurrent and progressive loss of OGTKO LV contractility (Fig. 8) in the absence of hypertrophy.

### **Increased NEDD4-1 and protein ubiquitination in the OGTKO are consistent with decreased $\text{Ca}_v$ expression and $I_{\text{Ca}}$**

Work by Rougier et al. suggested that NEDD4-1 overexpression regulates L-type  $\text{Ca}_v$ s by disrupting the exit of  $\text{Ca}_v$ s from the Golgi [56]. Here, studies into a potential role of endogenous NEDD4-1 in reducing OGTKO  $\text{Ca}_v$  activity and subunit expression indicated that NEDD4-1 levels and protein ubiquitination are elevated in OGTKO ventricles (Fig. 4d–f) but a direct relationship between these phenomena and the reduction in OGTKO  $\text{Ca}_v$ s has yet to be established. O-GlcNAcylation was specifically shown to limit protein degradation by blocking ubiquitination [42]; therefore, it is reasonable to predict increased ubiquitination in the absence of OGT. Studies investigating whether OGTKO  $\text{Ca}_v$  are retained in the Golgi or demonstrate differences in ubiquitination or interactions with ubiquitin-related proteins are currently ongoing but are, as of yet, inconclusive. A subsequent study by the same group also identified the de-ubiquitinating (dub) enzyme USP2 as a negative regulator of L-type  $\text{Ca}_v$ s [57] and O-GlcNAcylation was shown by other groups to regulate several dub proteins [58]. Dub proteins and ubiquitin ligases such as NEDD4-1 serve antagonizing roles in the ubiquitination process; thus, it is surprising that such proteins would have similar effects on  $\text{Ca}_v$  activity/expression. Although it is important to point out that the studies investigating the impact of NEDD4-1 and USP2 on the L-type  $\text{Ca}_v$  were performed in over-expression systems that likely do not recapitulate a native cardiomyocyte. The regulation of membrane proteins through ubiquitination and, ultimately, degradation is critically important as well as being exceedingly complex involving thousands of proteins [21]. Whether and how O-GlcNAcylation regulates ventricular myocyte  $\text{Ca}_v$  expression, and thereby  $I_{\text{Ca}}$  density, through an interplay with ubiquitination will require additional work; however, it is clear that OGT-gene deletion and, presumably, the subsequent reductions in O-GlcNAcylation, impact ubiquitin signaling as evidenced by the significant increase in ubiquitinated proteins in OGTKO hearts (Fig. 4e and f) suggesting an important link between these processes.

### **Potential mechanisms by which reduced O-GlcNAcylation impacts $\text{Ca}_v$ gating and results in increased adrenergic stimulation efficacy**

While alterations in the OGTKO NEDD4-1/ubiquitin pathway may well explain the reduced  $I_{\text{Ca}}$  density and  $\text{Ca}_v$  subunit expression levels, it is unlikely that this pathway can explain the additional observation of a rightward shift in OGTKO  $\text{Ca}_v$  steady-state-gating and window current or slowing of inactivation. Thus, we initially hypothesized that the depolarization of steady-state gating was caused through electrostatic mechanisms conferred by an increase in  $\text{Ca}_v$  subunit phosphorylation in the OGTKO. This speculation was based on the fact that O-GlcNAcylation often overlaps with phosphorylation where the same serine/threonine residue can be reciprocally modified [30] and cardiac  $\text{Ca}_v \alpha 1$  and  $\beta 2$  subunits are substrates of several kinases [23, 25, 51], and, as reported here for the first time, are O-GlcNAcylated under basal conditions in ventricular myocytes (Fig. 5). Thus, it is conceivable to infer conservation of the two modifications among some  $\alpha 1$  and  $\beta 2$  serine/threonine residues. Based on this, we rationalized that, in the absence of O-GlcNAcylation in OGTKO cardiomyocytes, the O-GlcNAcylation/phosphorylation equilibrium of  $\text{Ca}_v \alpha 1$  and  $\beta 2$  would shift toward increased phosphorylation. The impact of phosphorylation on cardiac  $\text{Ca}_v$  function can vary greatly depending on the kinases involved and the  $\text{Ca}_v$  subunits and residues that are phosphorylated with both increases and decreases in  $\text{Ca}_v$  activity being reported as well as rightward and leftward shifts in gating [7, 35, 37]. As one example, a phosphomimetic mutation in  $\text{Ca}_v \beta 2$  resulted in a decrease in  $\text{Ca}_v$  activity and a marked rightward shift in activation and inactivation gating [7]. However, we speculate that if increased  $\text{Ca}_v$  phosphorylation in the OGTKO contributes to the effect of reduced O-GlcNAcylation on  $\text{Ca}_v$  gating, it may not occur through any one specific phosphorylation pathway, but rather through a non-specific electrostatic mechanism. That is, as suggested by others [3, 27], a general increase in the number of negatively charged phosphate groups attached to the cytosolic portions of OGTKO  $\text{Ca}_v$  subunits, or other proteins in sufficiently close proximity, may effectively hyperpolarize the membrane potential sensed by the  $\text{Ca}_v$  voltage sensors, thereby requiring a greater depolarization for OGTKO  $\text{Ca}_v$  gating to occur as is observed (Fig. 2d). An investigation into the role of increased  $\text{Ca}_v$  phosphorylation in conditions of reduced O-GlcNAcylation and how this may impact channel function utilizing proteomic and pharmacologic approaches is necessary and ongoing. To this end, identifying the specific  $\text{Ca}_v \alpha 1$  and  $\beta 2$  residues that are O-GlcNAcylated and the phosphorylation pathways that are disrupted in the OGTKO will be of paramount

importance in resolving these questions. Alterations in  $\text{Ca}_v$  phosphorylation or signaling pathways that utilize phosphorylation may also contribute to the slowing of OGTKO  $\text{Ca}_v$  inactivation (Fig. 2e). However, because  $\text{Ca}^{2+}$  influx accelerates  $\text{Ca}_v$  inactivation [ $\text{Ca}^{2+}$ -dependent inactivation (CDI) [41]], under these experimental conditions, it is difficult to speculate a cause of the slowing of OGTKO  $\text{Ca}_v$  inactivation other than simply due to the reduced current (and thereby, reduced CDI). This is supported by the fact that the fast component of inactivation, which is largely thought to be ascribed to CDI [26], is impacted to a greater degree (~36% versus 14%; Fig. 2e and ST1) in OGTKO cardiomyocytes. This does not, however, rule out a direct effect on calmodulin, which is the  $\text{Ca}^{2+}$  sensor in CDI [49]. Additional experiments utilizing different intracellular  $\text{Ca}^{2+}$  concentrations and chelators or charge carriers (e.g.,  $\text{Ba}^{2+}$ ) will be required to explore this phenomenon more rigorously. Irrespective of the precise mechanism, the uniform rightward shifts in OGTKO  $\text{Ca}_v$  voltage-dependent steady-state gating and window current and the slowing of inactivation would be expected to confer a complex set of gains and losses of  $\text{Ca}_v$  function that would alter intracellular  $\text{Ca}^{2+}$  dynamics and, potentially, action potential duration [2]; these effects are all consistent with the significantly increased variability of EC coupling observed in OGTKO LV myocytes (Figs. 6e, 7a, b and e).

In addition to an interplay with ubiquitination and phosphorylation, O-GlcNAcylation was shown to affect protein function by modulating protein-to-protein interactions [67]. Therefore, an additional possible explanation for the reduction in OGTKO  $\text{Ca}_v$  activity and the shift in gating may stem from a disruption in the  $\text{Ca}_v$  complex, which could impact the stability of the channel. Additionally, evidence suggests an indispensable role for Rad, which is a member of the Rad and Gem/Kir Ras-related GTP-binding protein (RGK) family, in the regulation of cardiomyocyte  $\text{Ca}_v$  function. Under basal conditions, Rad inhibits  $\text{Ca}_v$  activity and, during adrenergic stimulation, Rad dissociates from  $\text{Ca}_v$ s removing its tonic inhibition [44]. Cardiomyocyte-specific deletion of the Rad gene resulted in an increase in  $\text{Ca}_v$  activity and a hyperpolarizing shift in activation gating [47]. Several RGK proteins are regulated by O-GlcNAcylation [43, 66], thus, given the data provided here, it is interesting to speculate a potential role for the regulation of  $\text{Ca}_v$ s by O-GlcNacylation that is mediated through Rad. If, for example, reductions in O-GlcNAcylation affect the expression of Rad or interaction of Rad with  $\text{Ca}_v$ s while also making Rad more susceptible to PKA phosphorylation during adrenergic stimulation, this could explain the effect of OGT gene deletion on  $\text{Ca}_v$  activity including the increased efficacy of adrenergic stimulation (Fig. 3). Preliminary studies into whether Rad expression is altered in the OGTKO and whether it

is O-GlcNAcylated have been hampered by the lack of a suitable Rad antibody but are ongoing.

### Potential pathophysiologic effects of altered O-GlcNAcylation on cardiac function

The reduction in OGTKO  $\text{Ca}_v$  activity was surprising in that some of the impetus for these studies was predicated on the fact that experimental models of diabetes/hyperglycemia were shown to result in reduced cardiomyocyte L-type  $\text{Ca}_v$  activity, with mechanisms largely unknown [45, 48, 63], while increased O-GlcNAcylation was shown to contribute to the pathologic molecular remodeling associated with diabetes [9, 19, 31, 50, 52, 53, 68]. An initial hypothesis, therefore, was that OGTKO  $\text{Ca}_v$  activity would be increased. If increased O-GlcNAcylation is involved in the reduction of  $\text{Ca}_v$  activity in diabetic models, there are several possible explanations for the apparent discrepancies between previous disease-related studies and our data here. As one example, there may be a multi-phasic effect of O-GlcNAc signaling on  $\text{Ca}_v$  activity in conditions of hyperglycemia. Others have also shown a protective effect of increased O-GlcNAcylation on cardiac function in that acute increases in O-GlcNAcylation, caused by the release of an unidentified humoral factor during a remote ischemic preconditioning intervention (rIPC), contributed to improved restoration of contractility following ischemia reperfusion injury [33]. Interestingly, the group also showed that diabetic patients, for whom O-GlcNAc levels would likely be higher under basal conditions due to the diabetes-related hyperglycemia, offered similar cardioprotection before rIPC but no additional protection after rIPC [33]. More specific models that link hyperglycemia, temporal increases in O-GlcNAcylation, and  $\text{Ca}_v$  function will be required to investigate these phenomena more rigorously. Pointedly, however, results from this study indicate that O-GlcNAcylation is a critical and direct regulator of cardiac  $\text{Ca}_v$  function; therefore, it is likely that in this model, where cardiomyocyte O-GlcNAcylation is drastically reduced and O-GlcNAc homeostasis is disrupted, a more severe phenotype is observed which is not fully reflective of diabetic/hyperglycemic disease-states where changes in O-GlcNAcylation would likely be more subtle and/or transient. Nevertheless, in addition to providing the first insight into this novel form of cardiac L-type  $\text{Ca}_v$  regulation, use of the OGTKO model, along with the development of more refined models that target individual  $\text{Ca}_v \alpha 1$  and  $\beta 2$  O-GlcNAcylation sites, should prove invaluable in elucidating the role of O-GlcNAcylation in mediating the effects of various signaling pathways that modulate  $\text{Ca}_v$  function in health and disease. Additionally, determining the impact of more transient changes in O-GlcNAc levels on  $\text{Ca}_v$  function should help uncover

how O-GlcNAcylation regulates  $Ca_v$  activity under basal conditions. Initial studies using glucosamine or OGA inhibitors, both of which can acutely increase O-GlcNAc levels, on isolated cardiomyocytes (1–6 h), indicated that such an approach is ineffective in modulating  $Ca_v$  function although this may be due to an inability to incubate adult mouse cardiomyocytes for a sufficient duration that alters  $Ca_v$  O-GlcNAcylation yet still allows for reliable  $I_{Ca}$  recordings.

It was previously shown in a similar model that ablation of the OGT-gene in adult mouse cardiomyocytes depressed cardiac function in non-stressed animals as evidenced by significantly reduced EF that onsets at approximately 4 weeks of age [65, 69]. Here we show that the deficits in OGTKO cardiac contractility (EF and to a larger extent FS) onset even earlier (19 dpi) with no indications of hypertrophy at the LV or myocyte levels (Figs. 2c and 8 and ST1 and ST2). Additionally, our data, as well as those from others, indicate that the reductions in ventricular contractility worsen over time along with an increase in systolic volume by 29 dpi (ST2) and an increase in diastolic volume by 2 months [65] suggesting dilation. Inducible cardiomyocyte OGT ablation was also shown to exacerbate the functional deterioration observed in pressure-overload and infarct models [10, 64, 69]. Several lines of questioning were investigated without identifying a causative mechanism. Our data here indicate for the first time that OGTKO LV myocyte  $Ca_v$  activity, intracellular  $Ca^{2+}$  release and contractility are all markedly reduced (Figs. 2, 6 and 7) by as early as 18 dpi (the earliest time-point tested). These data, therefore, suggest that diminished OGTKO cardiomyocyte EC coupling, largely resulting from a direct reduction in L-type  $Ca_v$  activity, plays a major role in the development of heart disease that likely progresses to heart failure, thus highlighting the critical role of O-GlcNAcylation in these processes as well as in the function of healthy and diseased hearts.

**Funding** This work was supported in part by grants from the National Science Foundation [Division of Molecular and Cellular Biosciences-1856199 to A.R.E and E.S.B., Division of Integrative Organismal Systems-1660926 to E.S.B.]; an American Heart Association Postdoctoral Fellowship (15POST25710010 to A.R.E]; and an American Heart Association Greater Southeast Affiliate Grant-In-Aid [14GRNT20450148 to E.S.B.].

**Availability of data and materials** All data and materials are available upon request.

## Compliance with ethical standard

**Conflict of interest** The authors declare that they have no conflict of interest or competing interests.

**Ethics approval** Animals were handled in accordance with the NIH Guide for the Care and Use of Laboratory Animals. All protocols

involving animals were approved by the Wright State University Institutional Animal Care and Use Committee (AUP 1163).

**Consent to participate** Not applicable.

**Consent for publication** All authors freely consent for publication.

**Code availability** Not applicable.

## References

1. Abele K, Yang J (2012) Regulation of voltage-gated calcium channels by proteolysis. *Sheng Li Xue Bao* 64:504–514
2. Alseikhan BA, DeMaria CD, Colecraft HM, Yue DT (2002) Engineered calmodulins reveal the unexpected eminence of  $Ca^{2+}$  channel inactivation in controlling heart excitation. *Proc Natl Acad Sci U S A.* 99:17185–17190. <https://doi.org/10.1073/pnas.262372999>
3. Ariyaratne A, Zocchi G (2015) Artificial phosphorylation sites modulate the activity of a voltage-gated potassium channel. *Phys Rev E Stat Nonlin Soft Matter Phys.* 91:032701. <https://doi.org/10.1103/physreve.91.032701>
4. Banerjee PS, Ma J, Hart GW (2015) Diabetes-associated dysregulation of O-GlcNAcylation in rat cardiac mitochondria. *Proc Natl Acad Sci U S A.* 112:6050–6055. <https://doi.org/10.1073/pnas.1424017112>
5. Bers DM, Grandi E (2009) Calcium/calmodulin-dependent kinase II regulation of cardiac ion channels. *J Cardiovasc Pharmacol* 54:180–187. <https://doi.org/10.1097/FJC.0b013e3181a25078>
6. Bersell K, Choudhury S, Mollova M, Polizzotti BD, Ganapathy B, Walsh S, Wadugu B, Arab S, Kuhn B (2013) Moderate and high amounts of tamoxifen in alphaMHC-MerCreMer mice induce a DNA damage response, leading to heart failure and death. *Dis Model Mech.* 6:1459–1469. <https://doi.org/10.1242/dmm.010447>
7. Brunet S, Emrick MA, Sadilek M, Scheuer T, Catterall WA (2015) Phosphorylation sites in the Hook domain of  $CaV\beta$  subunits differentially modulate  $CaV1.2$  channel function. *J Mol Cell Cardiol* 87:248–256. <https://doi.org/10.1016/j.jmcc.2015.08.006>
8. Bugger H, Abel ED (2014) Molecular mechanisms of diabetic cardiomyopathy. *Diabetologia* 57:660–671. <https://doi.org/10.1007/s00125-014-3171-6>
9. Clark RJ, McDonough PM, Swanson E, Trost SU, Suzuki M, Fukuda M, Dillmann WH (2003) Diabetes and the accompanying hyperglycemia impairs cardiomyocyte calcium cycling through increased nuclear O-GlcNAcylation. *J Biol Chem* 278:44230–44237. <https://doi.org/10.1074/jbc.M303810200>
10. Dassanayaka S, Brainard RE, Watson LJ, Long BW, Brittan KR, DeMartino AM, Aird AL, Gumpert AM, Audam TN, Kilfoil PJ, Muthusamy S, Hamid T, Prabhu SD, Jones SP (2017) Cardiomyocyte Ogt limits ventricular dysfunction in mice following pressure overload without affecting hypertrophy. *Basic Res Cardiol* 112:23. <https://doi.org/10.1007/s00395-017-0612-7>
11. De Jongh KS, Warner C, Colvin AA, Catterall WA (1991) Characterization of the two size forms of the alpha 1 subunit of skeletal muscle L-type calcium channels. *Proc Natl Acad Sci U S A.* 88:10778–10782. <https://doi.org/10.1073/pnas.88.23.10778>
12. Deng W, Ednie AR, Qi J, Bennett ES (2016) Aberrant sialylation causes dilated cardiomyopathy and stress-induced heart failure. *Basic Res Cardiol* 111:57. <https://doi.org/10.1007/s00395-016-0574-1>
13. Dubois-Deruy E, Belliard A, Mulder P, Bouvet M, Smet-Nocca C, Janel S, Lafont F, Beseme O, Amouyel P, Richard V, Pinet F (2015) Interplay between troponin T phosphorylation and

O-N-acetylglucosaminylation in ischaemic heart failure. *Cardiovasc Res* 107:56–65. <https://doi.org/10.1093/cvr/cvv136>

14. Ednie AR, Bennett ES (2015) Reduced sialylation impacts ventricular repolarization by modulating specific K<sup>+</sup> channel isoforms distinctly. *J Biol Chem* 290:2769–2783. <https://doi.org/10.1074/jbc.M114.605139>
15. Ednie AR, Deng W, Yip KP, Bennett ES (2019) Reduced myocyte complex N-glycosylation causes dilated cardiomyopathy. *FASEB J* 33:1248–1261. <https://doi.org/10.1096/fj.201801057R>
16. Ednie AR, Horton KK, Wu J, Bennett ES (2013) Expression of the sialyltransferase, ST3Gal4, impacts cardiac voltage-gated sodium channel activity, refractory period and ventricular conduction. *J Mol Cell Cardiol* 59:117–127. <https://doi.org/10.1016/j.jmcc.2013.02.013>
17. Ednie AR, Parrish AR, Sonner MJ, Bennett ES (2019) Reduced hybrid/complex N-glycosylation disrupts cardiac electrical signaling and calcium handling in a model of dilated cardiomyopathy. *J Mol Cell Cardiol* 132:13–23. <https://doi.org/10.1016/j.jmcc.2019.05.001>
18. Emmerich CH, Cohen P (2015) Optimising methods for the preservation, capture and identification of ubiquitin chains and ubiquitylated proteins by immunoblotting. *Biochem Biophys Res Commun* 466:1–14. <https://doi.org/10.1016/j.bbrc.2015.08.109>
19. Erickson JR, Pereira L, Wang L, Han G, Ferguson A, Dao K, Copeland RJ, Despa F, Hart GW, Ripplinger CM, Bers DM (2013) Diabetic hyperglycaemia activates CaMKII and arrhythmias by O-linked glycosylation. *Nature* 502:372–376. <https://doi.org/10.1038/nature12537>
20. Facundo HT, Brainard RE, Watson LJ, Ngoh GA, Hamid T, Prabhu SD, Jones SP (2012) O-GlcNAc signaling is essential for NFAT-mediated transcriptional reprogramming during cardiomyocyte hypertrophy. *Am J Physiol Heart Circ Physiol* 302:H2122–2130. <https://doi.org/10.1152/ajpheart.00775.2011>
21. Foot N, Henshall T, Kumar S (2017) Ubiquitination and the Regulation of Membrane Proteins. *Physiol Rev* 97:253–281. <https://doi.org/10.1152/physrev.00012.2016>
22. Fu Y, Xiao H, Zhang Y (2012) Beta-adrenoceptor signaling pathways mediate cardiac pathological remodeling. *Front Biosci (Elite Ed)* 4:1625–1637. <https://doi.org/10.2741/484>
23. Fuller MD, Emrick MA, Sadilek M, Scheuer T, Catterall WA (2010) Molecular mechanism of calcium channel regulation in the fight-or-flight response. *Sci Signal* 3:ra70. <https://doi.org/10.1126/scisignal.2001152>
24. Gao T, Puri TS, Gerhardstein BL, Chien AJ, Green RD, Hosey MM (1997) Identification and subcellular localization of the subunits of L-type calcium channels and adenylyl cyclase in cardiac myocytes. *J Biol Chem* 272:19401–19407. <https://doi.org/10.1074/jbc.272.31.19401>
25. Gerhardstein BL, Puri TS, Chien AJ, Hosey MM (1999) Identification of the sites phosphorylated by cyclic AMP-dependent protein kinase on the beta 2 subunit of L-type voltage-dependent calcium channels. *Biochemistry* 38:10361–10370. <https://doi.org/10.1021/bi990896o>
26. Grandi E, Morotti S, Ginsburg KS, Severi S, Bers DM (2010) Interplay of voltage and Ca-dependent inactivation of L-type Ca current. *Prog Biophys Mol Biol* 103:44–50. <https://doi.org/10.1016/j.pbiomolbio.2010.02.001>
27. Green WN, Andersen OS (1991) Surface charges and ion channel function. *Annu Rev Physiol* 53:341–359. <https://doi.org/10.1146/annurev.ph.53.030191.002013>
28. Haase H, Striessnig J, Holtzhauer M, Vetter R, Glossmann H (1991) A rapid procedure for the purification of cardiac 1,4-dihydropyridine receptors from porcine heart. *Eur J Pharmacol* 207:51–59. [https://doi.org/10.1016/s0922-4106\(05\)80037-9](https://doi.org/10.1016/s0922-4106(05)80037-9)
29. Hart GW (2014) Three decades of research on O-GlcNAcylation—a major nutrient sensor that regulates signaling, transcription and cellular metabolism. *Front Endocrinol (Lausanne)* 5:183. <https://doi.org/10.3389/fendo.2014.00183>
30. Hart GW, Slawson C, Ramirez-Correa G, Lagerlof O (2011) Cross talk between O-GlcNAcylation and phosphorylation: roles in signaling, transcription, and chronic disease. *Annu Rev Biochem* 80:825–858. <https://doi.org/10.1146/annurev-biochem-060608-102511>
31. Hu Y, Belke D, Suarez J, Swanson E, Clark R, Hoshijima M, Dillmann WH (2005) Adenovirus-mediated overexpression of O-GlcNAcase improves contractile function in the diabetic heart. *Circ Res* 96:1006–1013. <https://doi.org/10.1161/01.Res.0000165478.06813.58>
32. Ingham RJ, Gish G, Pawson T (2004) The Nedd4 family of E3 ubiquitin ligases: functional diversity within a common modular architecture. *Oncogene* 23:1972–1984. <https://doi.org/10.1038/sj.onc.1207436>
33. Jensen RV, Zachara NE, Nielsen PH, Kimose HH, Kristiansen SB, Bøtker HE (2013) Impact of O-GlcNAc on cardioprotection by remote ischaemic preconditioning in non-diabetic and diabetic patients. *Cardiovasc Res* 97:369–378. <https://doi.org/10.1093/cvr/cvs337>
34. Jiang K, Bai B, Ta Y, Zhang T, Xiao Z, Wang PG, Zhang L (2016) O-GlcNAc regulates NEDD4-1 stability via caspase-mediated pathway. *Biochem Biophys Res Commun* 471:539–544. <https://doi.org/10.1016/j.bbrc.2016.02.037>
35. Kamp TJ, Hell JW (2000) Regulation of cardiac L-type calcium channels by protein kinase A and protein kinase C. *Circ Res* 87:1095–1102. <https://doi.org/10.1161/01.res.87.12.1095>
36. Katchman A, Yang L, Zakharov SI, Kushner J, Abrams J, Chen BX, Liu G, Pitt GS, Colecraft HM, Marx SO (2017) Proteolytic cleavage and PKA phosphorylation of alpha1C subunit are not required for adrenergic regulation of CaV1.2 in the heart. *Proc Natl Acad Sci U S A* 114:9194–9199. <https://doi.org/10.1073/pnas.1706054114>
37. Keef KD, Hume JR, Zhong J (2001) Regulation of cardiac and smooth muscle Ca(2+) channels (Ca(V)1.2a, b) by protein kinases. *Am J Physiol Cell Physiol* 281:C1743–1756. <https://doi.org/10.1152/ajpcell.2001.281.6.C1743>
38. Kumari N, Gaur H, Bhargava A (2018) Cardiac voltage gated calcium channels and their regulation by beta-adrenergic signaling. *Life Sci* 194:139–149. <https://doi.org/10.1016/j.lfs.2017.12.033>
39. Laczy B, Marsh SA, Brocks CA, Wittmann I, Chatham JC (2010) Inhibition of O-GlcNAcase in perfused rat hearts by NAG-thiazolines at the time of reperfusion is cardioprotective in an O-GlcNAc-dependent manner. *Am J Physiol Heart Circ Physiol* 299:H1715–1727. <https://doi.org/10.1152/ajpheart.00337.2010>
40. Lang RM, Badano LP, Mor-Avi V, Afilalo J, Armstrong A, Ernande L, Flachskampf FA, Foster E, Goldstein SA, Kuznetsova T, Lancellotti P, Muraru D, Picard MH, Rietzschel ER, Rudski L, Spencer KT, Tsang W, Voigt JU (2015) Recommendations for cardiac chamber quantification by echocardiography in adults: an update from the American Society of Echocardiography and the European Association of Cardiovascular Imaging. *J Am Soc Echocardiogr* 28:1–39.e14. <https://doi.org/10.1016/j.echo.2014.10.003>
41. Lee KS, Marban E, Tsien RW (1985) Inactivation of calcium channels in mammalian heart cells: joint dependence on membrane potential and intracellular calcium. *J Physiol* 364:395–411. <https://doi.org/10.1113/jphysiol.1985.sp015752>
42. Li MD, Ruan HB, Hughes ME, Lee JS, Singh JP, Jones SP, Nitabach MN, Yang X (2013) O-GlcNAc signaling entrains the circadian clock by inhibiting BMAL1/CLOCK ubiquitination. *Cell Metab* 17:303–310. <https://doi.org/10.1016/j.cmet.2012.12.015>
43. Lima VV, Giachini FR, Hardy DM, Webb RC, Tostes RC (2011) O-GlcNAcylation: a novel pathway contributing to the effects of endothelin in the vasculature. *Am J Physiol Regul Integr Comp Physiol* 300:R111–R118. <https://doi.org/10.1152/ajpregu.00011.2011>

Physiol 300:R236–250. <https://doi.org/10.1152/ajpregu.00230.2010>

44. Liu G, Papa A, Katchman AN, Zakharov SI, Roybal D, Hennessey JA, Kushner J, Yang L, Chen BX, Kushner A, Dangas K, Gygi SP, Pitt GS, Colecraft HM, Ben-Johny M, Kalocsay M, Marx SO (2020) Mechanism of adrenergic CaV1.2 stimulation revealed by proximity proteomics. *Nature* 577:695–700. <https://doi.org/10.1038/s41586-020-1947-z>

45. Lu Z, Ballou LM, Jiang YP, Cohen IS, Lin RZ (2011) Restoration of defective L-type Ca<sup>2+</sup> current in cardiac myocytes of type 2 diabetic db/db mice by Akt and PKC-*ι*. *J Cardiovasc Pharmacol* 58:439–445. <https://doi.org/10.1097/FJC.0b013e318228e68c>

46. Luo B, Soesanto Y, McClain DA (2008) Protein modification by O-linked GlcNAc reduces angiogenesis by inhibiting Akt activity in endothelial cells. *Arterioscler Thromb Vasc Biol* 28:651–657. <https://doi.org/10.1161/atvba.107.159533>

47. Manning JR, Yin G, Kaminski CN, Magyar J, Feng HZ, Penn J, Sievert G, Thompson K, Jin JP, Andres DA, Satin J (2013) Rad GTPase deletion increases L-type calcium channel current leading to increased cardiac contraction. *J Am Heart Assoc* 2:e000459. <https://doi.org/10.1161/jaha.113.000459>

48. Pereira L, Matthes J, Schuster I, Valdivia HH, Herzig S, Richard S, Gomez AM (2006) Mechanisms of [Ca<sup>2+</sup>]<sub>i</sub> transient decrease in cardiomyopathy of db/db type 2 diabetic mice. *Diabetes* 55:608–615. <https://doi.org/10.2337/diabetes.55.03.06.db05-1284>

49. Peterson BZ, DeMaria CD, Adelman JP, Yue DT (1999) Calmodulin is the Ca<sup>2+</sup> sensor for Ca<sup>2+</sup>-dependent inactivation of L-type calcium channels. *Neuron* 22:549–558. [https://doi.org/10.1016/s0896-6273\(00\)80709-6](https://doi.org/10.1016/s0896-6273(00)80709-6)

50. Peterson SB, Hart GW (2016) New insights: a role for O-GlcNAcylation in diabetic complications. *Crit Rev Biochem Mol Biol* 51:150–161. <https://doi.org/10.3109/10409238.2015.1135102>

51. Puri TS, Gerhardstein BL, Zhao XL, Ladner MB, Hosey MM (1997) Differential effects of subunit interactions on protein kinase A- and C-mediated phosphorylation of L-type calcium channels. *Biochemistry* 36:9605–9615. <https://doi.org/10.1021/bi970500d>

52. Ramirez-Correa GA, Jin W, Wang Z, Zhong X, Gao WD, Dias WB, Vecoli C, Hart GW, Murphy AM (2008) O-linked GlcNAc modification of cardiac myofilament proteins: a novel regulator of myocardial contractile function. *Circ Res* 103:1354–1358. <https://doi.org/10.1161/circresaha.108.184978>

53. Ramirez-Correa GA, Ma J, Slawson C, Zeidan Q, Lugo-Fagundo NS, Xu M, Shen X, Gao WD, Caceres V, Chakir K, DeVine L, Cole RN, Marchionni L, Paolocci N, Hart GW, Murphy AM (2015) Removal of abnormal myofilament O-GlcNAcylation restores Ca<sup>2+</sup> sensitivity in diabetic cardiac muscle. *Diabetes* 64:3573–3587. <https://doi.org/10.2337/db14-1107>

54. Reeves RA, Lee A, Henry R, Zachara NE (2014) Characterization of the specificity of O-GlcNAc reactive antibodies under conditions of starvation and stress. *Anal Biochem* 457:8–18. <https://doi.org/10.1016/j.ab.2014.04.008>

55. Ren J, Gintant GA, Miller RE, Davidoff AJ (1997) High extracellular glucose impairs cardiac E-C coupling in a glycosylation-dependent manner. *Am J Physiol* 273:H2876–2883. <https://doi.org/10.1152/ajpheart.1997.273.6.H2876>

56. Rougier JS, Albesa M, Abriel H, Viard P (2011) Neuronal precursor cell-expressed developmentally down-regulated 4-1 (NEDD4-1) controls the sorting of newly synthesized Ca(V)1.2 calcium channels. *J Biol Chem* 286:8829–8838. <https://doi.org/10.1074/jbc.M110.166520>

57. Rougier JS, Albesa M, Syam N, Halet G, Abriel H, Viard P (2015) Ubiquitin-specific protease USP2-45 acts as a molecular switch to promote alpha2delta-1-induced downregulation of Cav1.2 channels. *Pflugers Arch* 467:1919–1929. <https://doi.org/10.1007/s00424-014-1636-6>

58. Ruan HB, Nie Y, Yang X (2013) Regulation of protein degradation by O-GlcNAcylation: crosstalk with ubiquitination. *Mol Cell Proteomics* 12:3489–3497. <https://doi.org/10.1074/mcp.R113.029751>

59. Seravalle G, Mancia G, Grassi G (2014) Role of the sympathetic nervous system in hypertension and hypertension-related cardiovascular disease. *High blood press. Cardiovasc Prev.* 21:89–105. <https://doi.org/10.1007/s40292-014-0056-1>

60. Sipido KR, Maes M, Van de Werf F (1997) Low efficiency of Ca<sup>2+</sup> entry through the Na(+)-Ca<sup>2+</sup> exchanger as trigger for Ca<sup>2+</sup> release from the sarcoplasmic reticulum. A comparison between L-type Ca<sup>2+</sup> current and reverse-mode Na(+)-Ca<sup>2+</sup> exchange. *Circ Res* 81:1034–1044. <https://doi.org/10.1161/01.res.81.6.1034>

61. Snow CM, Senior A, Gerace L (1987) Monoclonal antibodies identify a group of nuclear pore complex glycoproteins. *J Cell Biol* 104:1143–1156. <https://doi.org/10.1083/jcb.104.5.1143>

62. Trinidad JC, Barkan DT, Gullede BF, Thalhammer A, Sali A, Schoepfer R, Burlingame AL (2012) Global identification and characterization of both O-GlcNAcylation and phosphorylation at the murine synapse. *Mol Cell Proteomics* 11:215–229. <https://doi.org/10.1074/mcp.O112.018366>

63. Wang DW, Kiyosue T, Shigematsu S, Arita M (1995) Abnormalities of K<sup>+</sup> and Ca<sup>2+</sup> currents in ventricular myocytes from rats with chronic diabetes. *Am J Physiol* 269:H1288–1296. <https://doi.org/10.1152/ajpheart.1995.269.4.H1288>

64. Watson LJ, Facundo HT, Ngoh GA, Ameen M, Brainard RE, Lemma KM, Long BW, Prabhu SD, Xuan YT, Jones SP (2010) O-linked beta-N-acetylglucosamine transferase is indispensable in the failing heart. *Proc Natl Acad Sci U S A.* 107:17797–17802. <https://doi.org/10.1073/pnas.1001907107>

65. Watson LJ, Long BW, DeMartino AM, Britttian KR, Readnower RD, Brainard RE, Cummins TD, Annamalai L, Hill BG, Jones SP (2014) Cardiomyocyte Ogt is essential for postnatal viability. *Am J Physiol Heart Circ Physiol.* 306:H142–153. <https://doi.org/10.1152/ajpheart.00438.2013>

66. Wu W, Zheng X, Wang J, Yang T, Dai W, Song S, Fang L, Wang Y, Gu J (2018) O-GlcNAcylation on Rab3A attenuates its effects on mitochondrial oxidative phosphorylation and metastasis in hepatocellular carcinoma. *Cell Death Dis.* 9:970. <https://doi.org/10.1038/s41419-018-0961-7>

67. Yang X, Qian K (2017) Protein O-GlcNAcylation: emerging mechanisms and functions. *Nat Rev Mol Cell Biol* 18:452–465. <https://doi.org/10.1038/nrm.2017.22>

68. Yokoe S, Asahi M, Takeda T, Otsu K, Taniguchi N, Miyoshi E, Suzuki K (2010) Inhibition of phospholamban phosphorylation by O-GlcNAcylation: implications for diabetic cardiomyopathy. *Glycobiology* 20:1217–1226. <https://doi.org/10.1093/glycob/cwq071>

69. Zhu WZ, El-Nachef D, Yang X, Ledee D, Olson AK (2019) O-GlcNAc transferase promotes compensated cardiac function and protein kinase A O-GlcNAcylation during early and established pathological hypertrophy from pressure overload. *J Am Heart Assoc* 8:e011260. <https://doi.org/10.1161/jaha.118.011260>